Big Data and Computing Visions

www.bidacv.com

Big. Data. Comp. Vis. Vol. 4, No. 2 (2024) 95–109.

Paper Type: Original Article

A Shallow Convolutional Neural Network for Cerebral Neoplasm Detection from Magnetic Resonance Imaging

Hossein Sadr[1], Zeinab Khodaverdian[2], Mojdeh Nazari[1,*], Mohammad Reza Yamaghani[4]

[1] Health Informatics and Intelligent Systems Research Center, Guilan University of Medical Sciences, Rasht, Iran; hossein.sadr@gums.ac.ir.
[2] Department of Computer Engineering, Science and Research Branch, Islamic Azad University, Tehran, Iran; zeinab.khodaverdian@srbiau.ac.ir.
[3] Department of Health Information Technology and Management, School of Allied Medical Sciences, Shahid Beheshti University of Medical Sciences, Tehran, Iran; mojdeh.nazari@sbmu.ac.ir.
[4] Department of Computer Engineering, Lahijan Branch, Islamic Azad University, Lahijan, Iran; o_yamaghani@iau.ac.ir.

Citation:

Received: 21 Januray 2024 *Revised: 22 March 2024* *Accepted: 16 April 2024*	Sadr, H., Khodaverdian, Z., Nazari, M., & Yamaghani, M. R. (2024). A shallow convolutional neural network for cerebral neoplasm detection from magnetic resonance imaging. *Big data and computing visions, 4*(2), 95-109.

Abstract

The effective management of cerebral carcinoma relies on early and accurate diagnosis of brain cancers. Prompt diagnosis not only helps in developing more effective treatments but also has life-saving potential. Recently, machine learning algorithms have become increasingly important in medical imaging and information processing, offering a robust alternative to the time-consuming and error-prone manual diagnosis of brain tumors. One prominent approach in this area is the use of Convolutional Neural Networks (CNNs), which excel in extracting significant features from medical images. These features are then used to classify Magnetic Resonance Imaging (MRI) scans, determining the presence of neural tumors. Accordingly, a shallow CNN model is proposed in this paper to classify MRI scans. The proposed model was implemented on the brain tumor MRI dataset, and the results of experiments showed promise in enhancing the accuracy of brain tumor detection, ultimately leading to better patient outcomes. The result of this study not only enables healthcare professionals to quickly and accurately identify brain malignancies but also automates the diagnostic process and minimizes dependence on manual interpretation. This approach can potentially transform cerebral carcinoma diagnosis, making it more efficient and less prone to human error.

Keywords: Artificial intelligence, Machine learning, Deep learning, Cerebral neoplasm, Health care.

1 | Introduction

Brain tumors, identified as a significant health concern, impact individuals across all age groups. They constitute 85-90% of primary Central Nervous System (CNS) tumors, with approximately 11,700 new cases reported annually, highlighting the urgent need for advanced research and treatment [1]-[3]. These tumors,

Corresponding Author: mojdeh.nazari@sbmu.ac.ir
https://doi.org/10.22105/bdcv.2024.474574.1182
Licensee System Analytics. This article is an open access article distributed under the terms and conditions of the Creative Commons Attribution (CC BY) license (http://creativecommons.org/licenses/by/4.0).

characterized by abnormal tissue growth in the brain, disrupt normal brain functions and affect surrounding tissues. Detection of brain tumors relies heavily on their size and location, which presents a substantial diagnostic challenge [4], [5].

The diverse types of brain tumors, including benign, malignant, and pituitary tumors, each require distinct categorization and treatment strategies. Benign tumors, though not cancerous, can still cause serious health issues due to their size and location [6]. Malignant tumors, on the other hand, are cancerous and more aggressive, often leading to severe complications and requiring intensive treatment. Pituitary tumors, arising from the pituitary gland, can affect hormonal balance and require specialized diagnostic approaches [7], [8]. The tumor-affected area of the brain is shown in *Fig. 1*, which additionally determines the precise position of the infection within the brain.

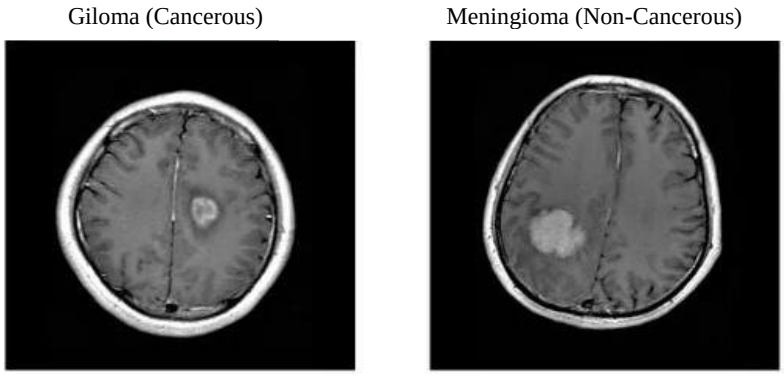

Fig. 1. Brain MRI's.

Effective management of brain tumors demands meticulous care, strategic treatment planning, and precise diagnostics [9], [10]. Among the various diagnostic tools available, Magnetic Resonance Imaging (MRI) stands out as the most reliable for detecting brain malignancies. MRI scans produce extensive sets of high-resolution images, allowing radiologists to analyze the brain's structure in great detail. This noninvasive imaging technique is crucial for evaluating, identifying, and classifying potential tumors, providing essential information for treatment planning [11].

Despite its effectiveness, the manual assessment of MRI scans is inherently labor-intensive and demands substantial medical expertise. Radiologists must carefully review the vast amount of image data, which can be prone to human error [12], [13].

An automatic and efficient brain tumor classification system aids physicians in interpreting medical images and assists specialists in making early-stage tumor growth decisions. Recently, the advent of advanced deep learning algorithms and their demonstrated effectiveness in addressing a range of challenges in artificial intelligence has significantly increased interest in health-related topics and algorithms. Numerous studies have explored the classification of different tumors through MRI, particularly MR brain images, employing artificial neural network algorithms [14], [15]. These studies have implemented various methods and found that shallow deep-learning algorithms can effectively differentiate between normal and abnormal brain MR images [16], [17]. Convolutional Neural Networks (CNNs) are highly recommended for image processing among the available methods due to their significant advancements [7], [18]. Therefore, the following solutions are presented in this work:

I. Proposing a shallow CNN architecture designed to extract relevant features for brain tumor classification automatically.

II. The proposed model achieves high accuracy in brain tumor classification.

III. By utilizing fewer trainable parameters, the suggested architecture reduces model complexity and enhances training efficiency.

The remainder of this paper is structured as follows. Section 2 reviews the relevant literature and related work. Section 3 details the proposed model. Section 4 outlines the experimental procedures and presents the

empirical results, including an analysis of why the proposed model outperforms others. And finally, Section 5 offers conclusions and discusses potential directions for future research.

2 | Literature Review

The use of digital imaging in the medical field is on the rise, with MRI playing a crucial role in the early detection and diagnosis of brain tumors due to its ability to produce detailed and high-contrast images of soft tissues. However, interpreting MRI scans is complex and time-consuming, requiring highly skilled professionals to recognize accurately and segment brain tumors [19]-[21].

Brain tumor detection from MRI images utilizes a combination of traditional methods, such as thresholding and machine learning, alongside emerging techniques like deep learning and hybrid approaches [22]. Brain Tumor Detection Techniques used in MRI Images are provided in *Fig. 2*.

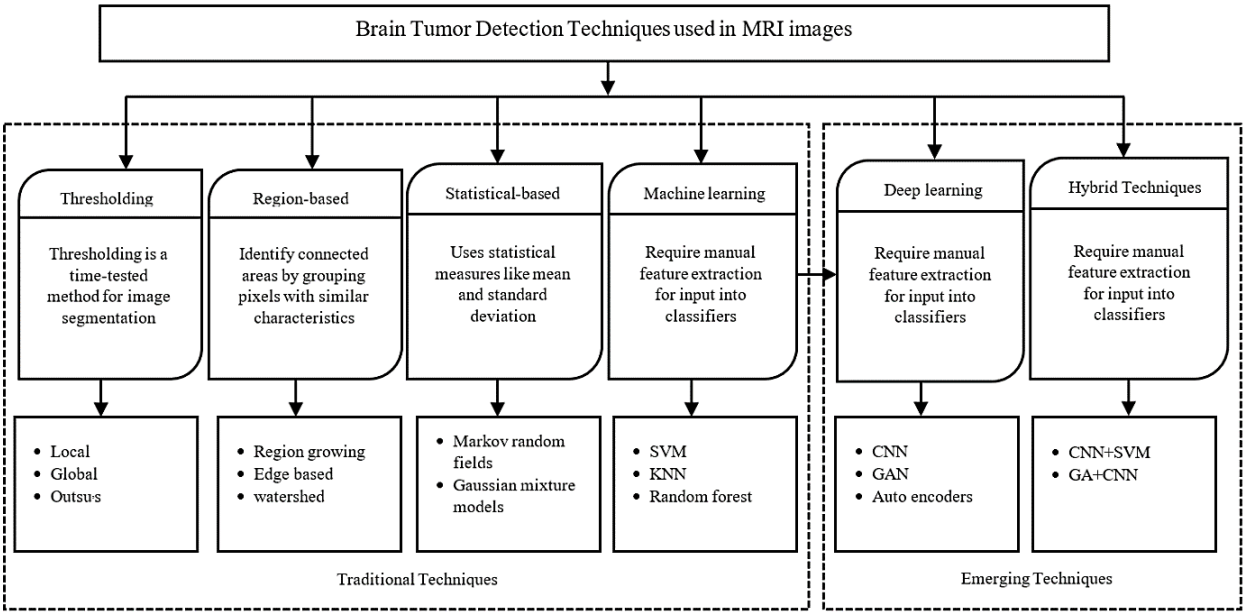

Fig. 2. Brain tumor detection techniques used in MRI images.

Thresholding is a time-tested method for image segmentation, where regions are differentiated based on intensity differences by comparing them to predefined threshold values [23], [24]. These thresholds, derived from local statistical properties such as mean intensity, help segment the image into distinct sections.

Region-based methods, on the other hand, identify connected areas by grouping pixels with similar characteristics, offering both simplicity and noise resistance. Similarly, statistical-based segmentation uses statistical measures like mean and standard deviation, making it well-suited for medical imaging [25]. Techniques such as Markov random fields, Gaussian mixture models, and expectation maximization rely on statistical parameters to effectively describe and segment images [26].

Computer-aided methods have been developed to enhance the accuracy of brain tumor classification. They can be categorized into semi-automated and fully automated systems to improve the accuracy of brain tumor classification. Semi-automated methods involve manual feature extraction for input into classifiers, while fully automated systems utilize deep learning algorithms, such as CNNs, to handle the entire process [27]. Furthermore, hybrid techniques, which combine two or more methods, aim to achieve superior results by leveraging the strengths of each technique to address the limitations of individual approaches. Despite advancements in segmentation algorithms, challenges remain in reliably detecting tumors due to their diverse appearance, size, shape, and structure [28]. This highlights the continuous need for improvements in the accurate segmentation and classification of tumor regions.

In light of the points mentioned, Anaraki et al. [29] proposed a method that combines CNNs with a Genetic Algorithm (GA) for the noninvasive classification of different grades of glioma using MRI. This approach achieved an accuracy of 90.9% in classifying the three grades of glioma.

Choudhury et al. [30] proposed a method for brain tumor detection and classification using CNNs and Deep Neural Networks (DNN). Their work serves as a foundation for applying deep learning techniques to brain tumor diagnosis.

In the work by Kumar et al. [31], three shallow CNNs were utilized alongside three pre-trained models: ResNet50, InceptionV3, and MobileNetV2 for brain tumor classification. The tumors were categorized into Meningioma, Glioma, and Pituitary. *Model (1)* achieved the highest accuracy at 98.47%, followed by *Model (2)* with an accuracy of 95.41%. Among the pre-trained models, InceptionV3 delivered the best performance with an accuracy of 92.36%.

Noh et al. [32] introduced a deconvolution network for semantic segmentation. Their work made an important contribution to the field of computer vision by learning the inverse mapping of CNNs, which is now a key idea in contemporary semantic segmentation models, to address pixel-wise labeling challenges.

Sasikala et al. [33] published a lung cancer detection and classification study. Their work advances the field of medical image analysis by showing how CNNs can reliably diagnose lung cancer, which is helpful for our research on related deep-learning applications in medical imaging.

Marco et al. [34] assessed seven deep CNN models for brain tumor classification. Their study included a generic CNN model as well as six pre-trained models. The models evaluated include Generic CNN, ResNet50, InceptionV3, InceptionResNetV2, Xception, MobileNetV2, and EfficientNetB0. Among these, InceptionV3 achieved the highest performance, with an average accuracy of 97.12%. The advancement of these techniques could significantly aid clinicians in the early detection of brain tumors.

Abd-Ellah et al. [35] conducted a comprehensive review of brain tumor diagnosis using MRI images, highlighting practical implications, key achievements, and lessons learned in the field. This review offers valuable insights into the state of the art in brain tumor diagnosis, serving as a foundational resource for our research.

Also, Haque et al. [36] introduces NeuroNet19, a DNN architecture built on the VGG19 backbone and enhanced with a novel Inverted Pyramid Pooling Module (IPPM). NeuroNet19 is trained on four brain tumor classes: Glioma, meningioma, no tumor, and pituitary tumors, and is tested on a public dataset of 7023 images. The research shows that NeuroNet19 achieves a top accuracy of 99.3%, precision, recall, and F1 scores of 99.2%, and a Cohen Kappa Coefficient (CKC) of 99%.

In Shah et al.'s [37] research, the EfficientNet-B0 model, a deep CNN, was optimized with custom layers for effective brain tumor classification and detection. Enhancing techniques improved image quality, and data augmentation was used to expand the dataset for better model training. The finetuned EfficientNet-B0 demonstrated superior performance, achieving a 98.87% accuracy in classification and detection, and outperformed other CNN models like VGG16, InceptionV3, Xception, ResNet50, and InceptionResNetV2 in comparative analyses.

Also, A hybrid CNN model was developed by Yildirim et al. [38] to classify glioma, meningioma, pituitary tumors, and normal brain MRI images. Features were extracted using pre-trained EfficientNetB0 and ShuffleNet, improved with color adjustments, and combined and reduced with mRMR before classification with an SVM. This model achieved an accuracy of 95.4%, surpassing previous models.

Lakshmi and Nagaraja Rao's [39] proposed model utilizes the Inception-v3 CNN for deep learning, which extracts multi-level features to enable early brain tumor detection. The model incorporates deep learning techniques and optimizes hyperparameters using the Adam Optimizer and a loss function to train the algorithm. The softmax classifier categorizes the images, achieving an accuracy of 99.34% on training data and 89% on validation data.

The proposed model, developed by Anaya-Isaza and Mera-Jiménez [40], leverages transfer learning from the ImageNet dataset and uses ResNet50, achieving an F1 detection score of 92.34%. This score was attained through implementing transfer learning within the proposed framework. Furthermore, the Kruskal-Wallis test confirms that this method significantly outperforms conventional approaches at a 0.05 significance level.

Bacanin et al. [41] addressed the computational challenges of optimizing CNN hyperparameters, which are vital for high accuracy, by proposing a metaheuristic approach utilizing a modified firefly algorithm. This method automates the optimization process, resulting in a system capable of classifying glioma grades from MRI images with an accuracy of 97.4%.

Ekong et al. [42] proposed a novel model that combines the Bayesian algorithm with depth-wise separable convolutions for accurate brain tumor classification and prediction. The model outperforms other state-of-the-art models, achieving a training accuracy of 99.03% and a validation accuracy of 94.32%, with strong F1-score, precision, and recall values.

Also, Fayaz et al. [43] introduces a brain MRI classification model that utilizes discrete wavelet transform and CNNs. The model includes preprocessing with a median filter, feature extraction through 3-level Harr wavelet decomposition, and classification using a CNN, achieving 99% accuracy and surpassing other advanced algorithms in practical use.

Saeedi et al. [1] conducted a study using a dataset of 3,264 MRI brain images, applying preprocessing and augmentation techniques before developing a 2D CNN and a convolutional auto-encoder network. The 2D CNN achieved a training accuracy of 96.47%, while the auto-encoder network reached 95.63%, outperforming machine learning methods like MLP and KNN. A summary of the existing studies is provided in *Table 1*.

Table 1. A summary of the existing studies.

Reference	Model	Data Type	Data Type	Result
Anaraki et al. [29]	GA+CNN	MRI images	Accuracy	90.9%
Kumar et al. [31]	ResNet50, InceptionV3, and MobileNetV2	MRI images	Accuracy	InceptionV3 delivered the best performance with an accuracy of 92.36%.
Sasikala et al. [33]	ResNet50, InceptionV3, InceptionResNetV2, Xception, MobileNetV2, and EfficientNetB0	MRI images	Accuracy	InceptionV3 achieved the highest performance, with an average accuracy of 97.12%.
Haque et al. [36]	NeuroNet19	MRI images	Accuracy, precision, recall, F1, and CKC	accuracy of 99.3%, with precision, recall, and F1 scores of 99.2% and a CKC of 99%.
Shah et al. [37]	EfficientNet-B0	MRI images	Accuracy	98.87%
Yildirim et al. [38]	EfficientNetB0 and ShuffleNet	MRI images	Accuracy	95.4%
Lakshmi and Nagaraja Rao [39]	The Inception-v3	MRI images	Accuracy	Accuracy of 99.34% on training data and 89% on validation data
Anaya-Isaza and Mera-Jiménez [40]	ResNet50	MRI images	F1 score	92.34%
Bacanin et al. [41]	Firefly algorithm +CNN	MRI images	Accuracy	97.4%

Table 1. Continued.

Reference	Model	Data Type	Data Type	Result
Fayaz et al. [43]	Wavelet transform+CNN	MRI images	accuracy	99.00%
Saeedi et al. [1]	2D CNN and a convolutional auto-encoder	MRI images	accuracy	2D CNN achieved a training accuracy of 96.47%, and the auto-encoder network reached 95.63%
Ekong et al. [42]	Bayesian algorithm with depth-wise separable convolutions	MRI images	F1 score	94.32%

3 | Methodology

Early detection of brain tumors is crucial, as accurate classification often necessitates a biopsy through brain surgery. A shallow, deep learning architecture has been proposed to improve the identification and classification of brain tumors. This architecture is designed to reduce the number of learnable parameters in the CNN, thereby enhancing the speed of model training. The proposed method aims to diagnose glioma, meningioma, pituitary gland tumors, and healthy brains from MRI, thereby increasing the accuracy of early-stage tumor detection. The diagram illustrating the proposed method is shown in *Fig. 3*.

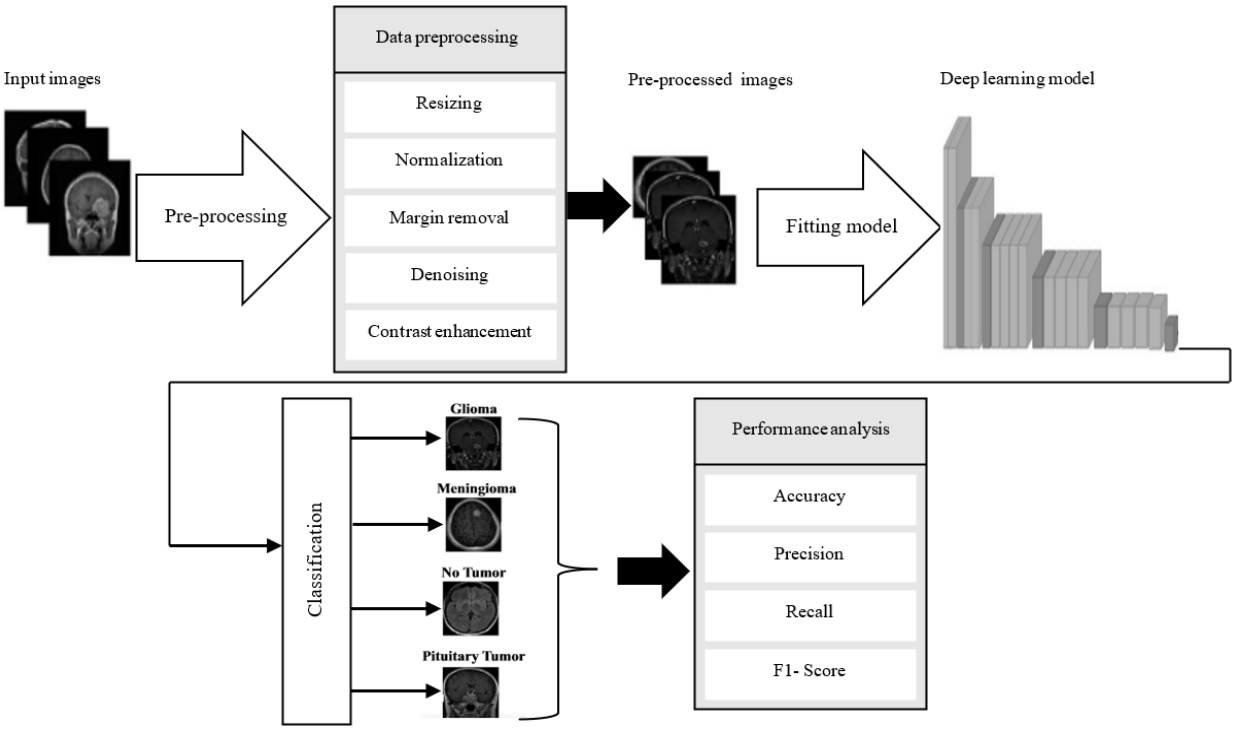

Fig. 3. Diagram of the proposed model.

Following this, the dataset used, input data preprocessing, the proposed model architecture, and its training will be described.

3.1 | Data Preprocessing

The input data preprocessing involves the following steps:

Step 1. Resizing: MRI images from the different sources-figshare, SARTAJ, and Br35H-are resized to a uniform dimension. This ensures consistency across the dataset and makes the images compatible with the deep-learning models.

Step 2. Normalization: the pixel intensity values of the images are normalized. This standardizes the pixel value range and improves the model's training efficiency and accuracy.

Step 3. Margin removal: any extra margins or borders around the MRI images are cropped. This step helps focus the analysis on the relevant brain regions and removes unnecessary background.

Step 4. Denoising: each image is processed with the Gaussian function for noise reduction, which applies the Gaussian blur effect. This method is similar to a non-uniform low-pass filter that reduces visual noise and extraneous details while preserving low spatial frequency components. Typically, this is accomplished by convolving the image with a Gaussian kernel [44] The mathematical representation of the Gaussian kernel is

$$G2D(\sigma, x, y) = \frac{1}{2\pi\sigma 2} e^{-\frac{x^2+y^2}{2\sigma^2}}.$$

In this equation, σ represents the standard deviation of the distribution, while x and y are the spatial coordinates. The value of σ determines the variance of the Gaussian distribution, which dictates the degree of blurring applied around each pixel.

Step 5. Contrast enhancement: contrast Limited Adaptive Histogram Equalization (CLAHE) is an advanced form of Adaptive Histogram Equalization (AHE) designed to prevent excessive contrast enhancement. Unlike traditional AHE processes the entire image simultaneously, CLAHE divides the image into smaller regions called tiles. It then reduces the artificial edges between these tiles by blending them using bi-linear interpolation. This method effectively enhances image contrast while avoiding over-amplification. CLAHE can also be applied to color images by focusing on the luminance channel in the Hue, Saturation, Value (HSV) color space. Applying CLAHE to only the luminance channel typically results in more effective contrast enhancement compared to adjusting all channels in a BGR image [45].

These preprocessing steps are tailored to address this dataset's specific challenges and characteristics, ensuring it is well-prepared for effective deep-learning analysis.

3.2 | Shallow CNN Model

CNN is created during the training stage of a brain neoplasm detection project from MRI utilizing CNN and ML models. It receives a tagged collection of MRI pictures with cancers identified in them. The CNN develops an understanding of the patterns and characteristics linked to neoplasms. The model tunes its internal parameters to reduce classification mistakes using backpropagation and optimization algorithms during training. The dataset is frequently split into training and training and validation sets to assess the model's effectiveness. The process iteratively continues as hyperparameters are adjusted until the model exhibits precise tumor detection abilities on unobserved data, enabling it to predict tumor presence or absence in new MRI pictures. This section outlines the structure of a CNN and its key components.

Convolution layer: the convolution layer serves as the foundational element of any CNN, giving the network its name. This layer contains kernels, typically square matrices whose values are learned during training. Unlike matrix multiplication, this layer uses convolution operations, which are mathematically expressed as follows [46]:

$$F(I, j) = (I * K)(I, j) = \sum m \sum n I(i + m, j + n) K(m, n),$$

where I represents the image, K is the 2D filter, and F is the resulting feature map. The dimensions of K are $m \times n$. CNNs detect local features in images common across the dataset or in a significant portion. These local features play a crucial role in image classification. The convolution layer identifies these features, and the output of this process is the feature map. Nonlinearity is introduced by passing the output of each convolutional layer through an activation function.

Pooling layer: the pooling layer progressively reduces the spatial dimensions of the feature maps from the convolution layers while retaining the most critical information. This reduction decreases the number of

parameters and computations in the network. Pooling is defined by a window of size wp×wp that moves with a stride stp across each feature map. There are two primary pooling methods [47]:

I. Max-pooling: returns the maximum value within each pooling window.

II. Avg-pooling: returns the average value within each pooling window.

Flatten layer: flattening converts the multidimensional data into a one-dimensional array, preparing it as input for the next layer. The output of the convolutional layers is flattened to form a continuous feature vector. This flattened vector is then passed to the final classification model, commonly known as the Fully Connected (FC) layer [48].

FC Layer: the FC layer, also known as the dense layer, connects every neuron in the current layer to every neuron in both the previous and subsequent layers. The number of neurons in this layer typically aligns with the number of categories or classes the network is designed to classify. Each neuron in the FC layer contributes to the final classification decision by integrating information from the preceding layers. The output of this layer is a vector with KKK dimensions, representing the probability of each class. The FC layer links the identified features to the final classification output, with higher values in the vector indicating the presence of specific objects in the image [49].

Dropout: dropout is a regularization technique used to prevent overfitting during the training of neural networks. It involves randomly setting a fraction of the neurons in a layer to zero during each training iteration. This random deactivation prevents the network from becoming too reliant on specific neurons and forces it to learn more robust features that are less dependent on any single neuron. The dropout rate, denoted as pp, determines the proportion of neurons to be dropped. For instance, a dropout rate of 0.5 means that half of the neurons are randomly turned off during each training pass. During inference or testing, dropout is turned off, and the full network is used to make predictions. This technique helps improve the model's generalization by reducing its tendency to overfit the training data [50].

Based on the outlined details, the proposed architecture for tumor detection is designed as follows:

The input images were resized to 150x150 pixels and processed through an initial Convolutional layer featuring 32 filters of size 3x3 and ReLU activation. This layer extracted basic image features. Two additional Convolutional layers with 64 filters each and ReLU activation were added to enhance feature extraction. The feature maps underwent down-sampling through a Max Pooling layer with a 2x2 pool size, which reduced computational load and supported spatial abstraction. Dropout layers with a rate of 0.3 were included after these stages to mitigate overfitting.

The architecture then incorporated two more convolutional layers, each with 64 filters, followed by a Max Pooling layer and an additional Dropout layer. This sequence was repeated to capture more complex features and improve the model's ability to detect detailed patterns in MRI images.

To further deepen the network and enhance feature representation, two sets of convolutional layers with 128 filters each were added, along with Max Pooling layers and Dropout layers, to regularize the network and facilitate the detection of complex cerebral neoplasm structures.

Subsequently, a convolutional layer with 256 filters and ReLU activation was introduced, followed by another Max Pooling layer and Dropout layer. This configuration enabled the network to capture higher-level and more abstract features.

The feature maps were flattened into a 1D vector and processed through two FC (Dense) layers: the first with 512 units and ReLU activation and the second with another 512 units and ReLU activation. These dense layers were crucial for data classification and understanding intricate relationships within the data.

The final output layer consisted of 4 neurons with softmax activation and a final Dropout layer set at a rate of 0.3 to reduce further overfit. This configuration allowed the model to output probability distributions for the four classes associated with cerebral neoplasm detection.

4 | Experiments

In this section, the dataset used in the experiment is first described. The subsequent section details the preprocessing steps applied to the dataset images for model training. The third section explains the performance metrics used to evaluate the model. The experiments conducted with the dataset are covered in the fourth section. The final section presents the results obtained from the experiments.

4.1 | Dataset

The dataset used in this research integrates three separate sources: figshare, SARTAJ, and Br35H, which includes 7022 MRI images [51]. These images are divided into four groups: glioma (1321 images for training and 300 images for testing), meningioma (1339 images for training and 306 images for testing), no tumor (1595 images for training and 405 images for testing), and pituitary (1457 images for training and 300 images for testing) are categorized. MRI images vary in size and need to be resized to uniform dimensions to ensure consistency in analysis. This resizing process and edge removal are critical to improving the accuracy of deep learning models used for classification.

The figshare dataset includes images collected in recent years from various contributors, while the SARTAJ dataset, collected in 2017 by the SARTAJ research group, has been found to be problematic due to inaccuracy in classifying glioma images. This issue was observed through the discrepancy in the results of different models and research. As a corrective measure, images from the figshare repository replaced problematic images from the SARTAJ dataset to ensure more reliable classification results. The Br35H dataset, containing images from tumor-free patients, was made available by researchers working on brain MRI diagnostics. Additionally, images from this dataset were acquired using different imaging protocols, contributing to image quality and appearance variations. Addressing these changes through preprocessing is necessary to achieve better model performance. Examples from the four classes in the dataset are shown in *Fig. 4*, and details are provided in *Table 2*.

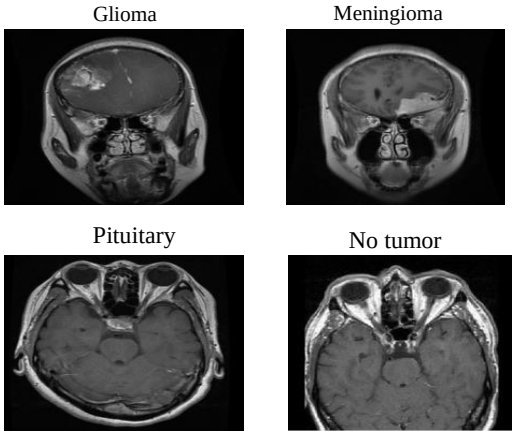

Fig. 4. Examples from the four classes in the dataset.

Table 2. Dataset details.

Classes	Training Samples	Test Samples
Glioma	1321	300
Meningioma	1339	306
No-tumor	1595	405
Pituitary	1457	300
Total	5712	1311

4.2 | Performance Metrics

The following metrics are used to evaluate our proposed model in comparison with other models:

Accuracy: accuracy measures the proportion of correct predictions made by the model or the likelihood that a given input is classified correctly. For each class, accuracy is calculated as

$$\text{Accuracy} = \frac{\text{Number of correctly predicted instances of the class}}{\text{Total number of instances of the class}}.$$

Precision: precision measures the proportion of positive identifications that are correctly classified. It is particularly useful for imbalanced datasets and is calculated as follows:

$$\text{Precision} = \frac{\text{True Positives}}{\text{Total Predicted Positives}}.$$

Recall: recall estimates the proportion of actual positives that are correctly identified. It is also useful for imbalanced datasets and is given by

$$\text{Recall} = \frac{\text{True Positives}}{\text{Total Actual}}.$$

F1-Score: F1-Score provides a balance between precision and recall and is especially useful for imbalanced datasets. It is the harmonic mean of precision and recall, calculated as

$$\text{F1} - \text{Score} = \frac{2 \times \text{Precision} \times \text{Recall}}{\text{Precision} + \text{Recall}}.$$

4.3 | Preprocess and Training

The preprocessing of the images involves several steps: first, three-channel images are converted to single-channel grayscale images. The images are then smoothed using Gaussian Blur with a 3x3 window size and a standard deviation 0. Next, CLAHE is applied to enhance the images and reduce noise, with a clip limit of 2 and a tile grid size of 8x8. This is followed by thresholding to remove noise through erosion and dilation operations, where pixels with grayscale values below 45 are set to 0. The contours of the images are determined, and the images are cropped accordingly. The cropped images are resized to 200x200 pixels for model training and testing. Finally, the classes of the images are encoded using one-hot encoding based on the folder to which each image belongs. The visual results of these processes are illustrated in *Fig. 5*. The images and their preprocessed versions are displayed, with the original images on the left, the Gaussian Blur-processed images in the center, and the CLAHE-treated images on the right. The first row features glioma class images; the second row shows meningioma class images; the third row represents no tumor class images, and the final row contains pituitary class images.

Subsequently, the dataset is divided according to the 5-fold cross-validation method for training the model. All programs are implemented using Python and TensorFlow. The Adam Optimizer is utilized to train the proposed model. Training the model is run for 20 epochs with a batch size of 24. The learning rate for the optimizer is set to 0.0001, with all other parameters left at their default values. Categorical cross-entropy is employed as the loss function during the training.

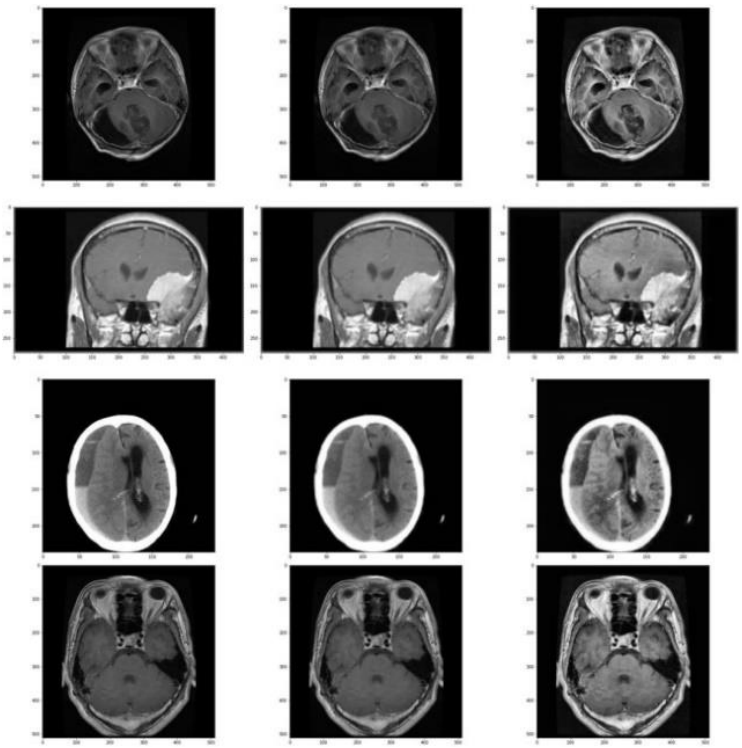

Fig. 5. Pre-processed data.

4.4 | Experimental Results

This section provides the empirical results investigating the efficiency of our proposed model in brain tumor classification. The proposed model was trained using 5-fold cross-validation, and *Table 3* includes the classification of our proposed shallow convolutional model based on all evaluation metrics. As can be seen, prediction accuracies of 95.23%, 94.89%, 95.32 %, and 95.69% are attained for glioma, meningioma, no tumor, and pituitary tumors, respectively. The average prediction accuracy is about 95.27%.

Additionally, the model achieved an average precision of 93%, a recall of 93%, and an F1-score of 0.93. The false-positive rate is close to 0, while the true negative rate is near 1, showcasing the exceptional efficiency of the Shallow CNN architecture. The Roc curve of the shallow CNN is also depicted in Figure 6. Upon analyzing the ROC curve, it is evident that the area under the curve is about 0.989, suggesting our model's robustness and broad applicability.

Table 3. Performance metrics of shallow CNN.

Tumor class	Accuracy (std)	Precision	Recall	FPR	TNR	F1-Score
Glioma	95.23% (0.07)	0.91	0.90	0.02	0.87	0.91
Meningioma	94.89% (0.11)	0.92	0.92	0. 01	0.86	0.95
No-tumor	95.32% (0.06)	0.93	0.91	0.00	0.89	0.97
Pituitary	95.69% (0.06)	0.91	0.91	0.00	0.89	0.94
Total	95.27%	0.93	0.90	0.01	0.87	0.95

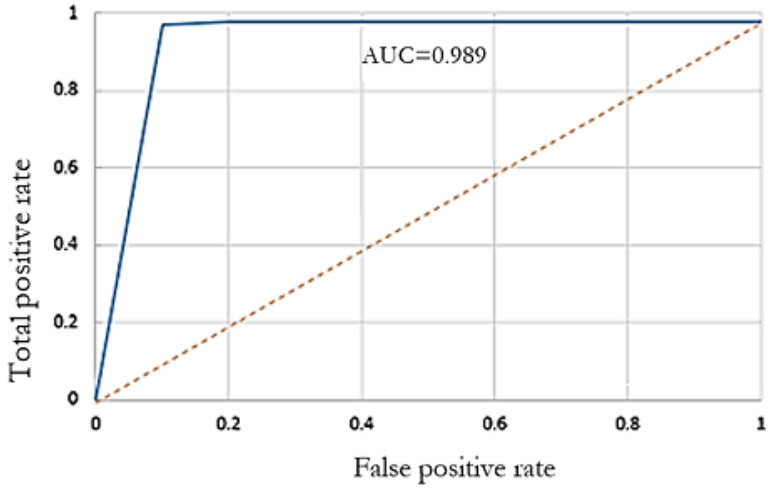

Fig. 7. ROC curve of the proposed 'shallow CNN'.

For better analysis, the computational complexity of our proposed model is also reported in *Table 4*. The computational cost is represented as a percentage, starting with CPU and GPU usage, then the percentage of CPU memory utilized, and finally, addressing the training time because of its connection to the overall computational cost. As seen, shallow CNN does not need many parameters and training time despite its great performance.

Table 4. Computational complexity evaluation.

Parameters	%CPU Utilization	%GPU Utilization	%GPU Memory Allocated	Training Time (Minutes)
3.5	73.45	40.49	32.95	200

One of the challenges of this study is locating a suitable dataset for the classification problem. Gathering current medical data can be quite difficult; however, platforms like Kaggle provide valuable resources for storing research datasets. Additionally, there is the issue of computational complexity. Utilizing cloud-based solutions, such as the free version of Google Colab, can be advantageous for performing these tasks. While obtaining a professional version could improve efficiency and resource management, it would necessitate access to a high-performance computer for effective research execution.

5 | Conclusion

The study presents a novel approach using shallow CNNs to detect cerebral neoplasms from MRI. Our experiments demonstrate that even shallow architectures can achieve competitive accuracy in identifying brain tumors, highlighting the potential for simplified models to contribute to effective diagnostic tools. The reduced computational complexity and shorter training times of shallow CNNs make them particularly advantageous for clinical settings where rapid decision-making is crucial.

Moreover, the positive results obtained from our model suggest that this method could enhance early detection and treatment planning for patients with brain tumors, ultimately improving clinical outcomes. Future work will further optimize the model and conduct extensive validations across diverse datasets to ensure robustness and generalizability. By integrating this technology into clinical practice, we can move towards more efficient and reliable diagnostics in the fight against cerebral neoplasms.

References

[1] Saeedi, S., Rezayi, S., Keshavarz, H., & R. Niakan Kalhori, S. (2023). MRI-based brain tumor detection using convolutional deep learning methods and chosen machine learning techniques. *BMC medical informatics and decision making*, *23*(1), 16. DOI: 10.1186/s12911-023-02114-6

[2] Zadeh Shirazi, A., Fornaciari, E., McDonnell, M. D., Yaghoobi, M., Cevallos, Y., Tello-Oquendo, L., … & Gomez, G. A. (2020). The application of deep convolutional neural networks to brain cancer images: a survey. *Journal of personalized medicine*, *10*(4), 224. DOI: 10.3390/jpm10040224

[3] Saberi, Z. A., Sadr, H., & Yamaghani, M. R. (2024). An intelligent diagnosis system for predicting coronary heart disease. *2024 10th international conference on artificial intelligence and robotics (QICAR)* (pp. 131–137). IEEE. DOI: 10.1109/QICAR61538.2024.10496601

[4] Ahmad, N., Thakur, R. S., & Khan, A. (2024). Brain tumor detection from magnetic resonance imaging images using shallow convolutional neural network. In *Deep learning applications in translational bioinformatics* (pp. 65–77). Academic Press. DOI: 10.1016/B978-0-443-22299-3.00005-0

[5] Khodaverdian, Z., Sadr, H., Edalatpanah, S. A., & Nazari, M. (2024). An energy aware resource allocation based on combination of CNN and GRU for virtual machine selection. *Multimedia tools and applications*, *83*(9), 25769–25796. DOI: 10.1007/s11042-023-16488-2

[6] Anagun, Y. (2023). Smart brain tumor diagnosis system utilizing deep convolutional neural networks. *Multimedia tools and applications*, *82*(28), 44527–44553. DOI: 10.1007/s11042-023-15422-w

[7] Kshatri, S. S., & Singh, D. (2023). Convolutional neural network in medical image analysis: a review. *Archives of computational methods in engineering*, *30*(4), 2793–2810. DOI: 10.1007/s11831-023-09898-w

[8] Sadr, H., Khodaverdian, Z., Nazari Soleimandarabi, M., & Edalatpanah, S. A. (2023). Virtual machine workload prediction to reduce energy consumption in cloud data centers using combination of deep learning models. *Journal of information and communication technology*, *55*(56), 166-189. (**In Persian**). magiran.com/p2613921

[9] Krishnapriya, S., & Karuna, Y. (2023). A survey of deep learning for MRI brain tumor segmentation methods: Trends, challenges, and future directions. *Health and technology*, *13*(2), 181–201. DOI: 10.1007/s12553-023-00737-3

[10] Zahmatkesh Zakariaee, A., Sadr, H., & Yamaghani, M. R. (2023). A new hybrid method to detect risk of gastric cancer using machine learning techniques. *Journal of AI and data mining*, *11*(4), 505-515. (**In Persian**). DOI: 10.22044/jadm.2023.13377.2464

[11] Hardaha, S., Edla, D. R., & Parne, S. R. (2023). A survey on convolutional neural networks for MRI analysis. *Wireless personal communications*, *128*(2), 1065–1085. DOI: 10.1007/S11277-022-09989-0

[12] Patil, S., & Kirange, D. (2023). Ensemble of deep learning models for brain tumor detection. *Procedia computer science*, *218*, 2468–2479. DOI: 10.1016/j.procs.2023.01.222

[13] Sadr, H., & Nazari Soleimandarabi, M. (2022). ACNN-TL: attention-based convolutional neural network coupling with transfer learning and contextualized word representation for enhancing the performance of sentiment classification. *The journal of supercomputing*, *78*(7), 10149–10175. DOI: 10.1007/s11227-021-04208-2

[14] Panigrahi, A., & Subasi, A. (2023). Magnetic resonance imagining-based automated brain tumor detection using deep learning techniques. In *Applications of artificial intelligence in medical imaging* (pp. 75–107). Elsevier. DOI: 10.1016/B978-0-443-18450-5.00012-8

[15] Kalashami, M. P., Pedram, M. M., & Sadr, H. (2022). EEG feature extraction and data augmentation in emotion recognition. *Computational intelligence and neuroscience*, *2022*(1), 7028517. DOI: 10.1155/2022/7028517

[16] Satyanarayana, G., Naidu, P. A., Desanamukula, V. S., & Rao, B. C. (2023). A mass correlation based deep learning approach using deep convolutional neural network to classify the brain tumor. *Biomedical signal processing and control*, *81*, 104395. DOI: 10.1016/j.bspc.2022.104395

[17] Sadr, H., Soleimandarabi, M. N., Pedram, M., & Teshnelab, M. (2019). Unified topic-based semantic models: a study in computing the semantic relatedness of geographic terms. *2019 5th international conference on web research* (ICWR) (pp. 134–140). IEEE. DOI: 10.1109/ICWR.2019.8765257

[18] Jadidinejad, A. H., & Sadr, H. (2015). Improving weak queries using local cluster analysis as a preliminary framework. *Indian journal of science and technology*, *8*(5), 495–510. DOI: 10.17485/ijst/2015/v8i15/46754

[19] Gelenbe, E., Feng, Y., & Krishnan, K. R. R. (1996). Neural network methods for volumetric magnetic resonance imaging of the human brain. *Proceedings of the IEEE*, *84*(10), 1488–1496. DOI: 10.1109/5.537113

[20] Sadr, H., Nazari, M., Pedram, M. M., & Teshnehlab, M. (2019). Exploring the efficiency of topic-based models in computing semantic relatedness of geographic terms. *International journal of web research*, *2*(2), 23–35. (**In Persian**) DOI: 10.22133/ijwr.2020.225866.1056

[21] Sadr, H., Pedram, M. M., & Teshnehlab, M. (2020). Multi-view deep network: a deep model based on learning features from heterogeneous neural networks for sentiment analysis. *IEEE access*, *8*, 86984–86997. DOI: 10.1109/ACCESS.2020.2992063

[22] Kanumuri, C., & Madhavi, C. H. R. (2022). A survey: brain tumor detection using MRI image with deep learning techniques. In *Smart and sustainable approaches for optimizing performance of wireless networks: real-time applications* (pp. 125–138). Wiley. DOI: 10.1002/9781119682554.ch6

[23] Avants, B. B., Tustison, N. J., Song, G., Cook, P. A., Klein, A., & Gee, J. C. (2011). A reproducible evaluation of ANTs similarity metric performance in brain image registration. *Neuroimage*, *54*(3), 2033–2044. DOI: 10.1016/j.neuroimage.2010.09.025

[24] Sadr, H., Pedram, M. M., & Teshnehlab, M. (2019). A robust sentiment analysis method based on sequential combination of convolutional and recursive neural networks. *Neural processing letters*, *50*, 2745–2761. DOI: 10.1007/s11063-019-10049-1

[25] Benson, C. C., Lajish, V. L., & Rajamani, K. (2015). Brain tumor extraction from mri brain images using marker based watershed algorithm. 2*015 international conference on advances in computing, communications and informatics (ICACCI).* (pp. 318–323). IEEE. https://ieeexplore.ieee.org/abstract/document/7275628/

[26] Held, K., Kops, E. R., Krause, B. J., Wells, W. M., Kikinis, R., & Muller-Gartner, H. W. (1997). Markov random field segmentation of brain MR images. *IEEE transactions on medical imaging*, *16*(6), 878–886. https://arxiv.org/pdf/0903.3114

[27] Iqbal, S., Ghani, M. U., Saba, T., & Rehman, A. (2018). Brain tumor segmentation in multi-spectral MRI using convolutional neural networks (CNN). *Microscopy research and technique*, *81*(4), 419–427. DOI: 10.1002/jemt.22994

[28] Havaei, M., Davy, A., Warde-Farley, D., Biard, A., Courville, A., Bengio, Y., … & Larochelle, H. (2017). Brain tumor segmentation with deep neural networks. *Medical image analysis*, *35*, 18–31. https://arxiv.org/pdf/1505.03540

[29] Anaraki, A. K., Ayati, M., & Kazemi, F. (2019). Magnetic resonance imaging-based brain tumor grades classification and grading via convolutional neural networks and genetic algorithms. *Biocybernetics and biomedical engineering*, *39*(1), 63–74. DOI: 10.1016/j.bbe.2018.10.004

[30] Choudhury, C. L., Mahanty, C., Kumar, R., & Mishra, B. K. (2020). Brain tumor detection and classification using convolutional neural network and deep neural network. *2020 international conference on computer science, engineering and applications (ICCSEA).* (pp. 1–4). IEEE. DOI: 10.1109/ICCSEA49143.2020.9132874

[31] Shukla, S. K., & Shukla, S. (2021). Shallow convolution neural network for brain tumor classification using t1-weighted mri scans. *2021 IEEE 2nd international conference on electrical power and energy systems (ICEPES)* (pp. 1–4). IEEE. DOI: 10.1109/ICEPES52894.2021.9699806

[32] Noh, H., Hong, S., & Han, B. (2015). Learning deconvolution network for semantic segmentation. *Proceedings of the ieee international conference on computer vision* (pp. 1520–1528). CVF.

[33] Sasikala, S., Bharathi, M., & Sowmiya, B. R. (2018). Lung cancer detection and classification using deep CNN. *International journal of innovative technology and exploring engineering (IJITEE)*, *8*(2S). https://www.ijitee.org/wp-content/uploads/papers/v8i2s/BS2713128218.pdf

[34] Gómez-Guzmán, M. A., Jiménez-Beristaín, L., García-Guerrero, E. E., López-Bonilla, O. R., Tamayo-Perez, U. J., Esqueda-Elizondo, J. J., ... & Inzunza-González, E. (2023). Classifying brain tumors on magnetic resonance imaging by using convolutional neural networks. *Electronics*, *12*(4), 955. DOI: 10.3390/electronics12040955

[35] Abd-Ellah, M. K., Awad, A. I., Khalaf, A. A. M., & Hamed, H. F. A. (2019). A review on brain tumor diagnosis from MRI images: practical implications, key achievements, and lessons learned. *Magnetic resonance imaging*, *61*, 300–318. DOI: 10.1016/j.mri.2019.05.028

[36] Haque, R., Hassan, M. M., Bairagi, A. K., & Shariful Islam, S. M. (2024). NeuroNet19: an explainable deep neural network model for the classification of brain tumors using magnetic resonance imaging data. *Scientific reports*, *14*(1), 1524. https://www.nature.com/articles/s41598-024-51867-1

[37] Shah, H. A., Saeed, F., Yun, S., Park, J. H., Paul, A., & Kang, J. M. (2022). A robust approach for brain tumor detection in magnetic resonance images using finetuned efficientNet. *IEEE access*, *10*, 65426–65438. DOI: 10.1109/ACCESS.2022.3184113

[38] Yildirim, M., Cengil, E., Eroglu, Y., & Cinar, A. (2023). Detection and classification of glioma, meningioma, pituitary tumor, and normal in brain magnetic resonance imaging using deep learning-based hybrid model. *Iran journal of computer science*, *6*(4), 455–464. DOI: 10.1007/s42044-023-00139-8

[39] Lakshmi, M. J., & Nagaraja Rao, S. (2022). Brain tumor magnetic resonance image classification: a deep learning approach. *Soft computing*, *26*(13), 6245–6253. DOI: 10.1007/s00500-022-07163-z

[40] Anaya-Isaza, A., & Mera-Jiménez, L. (2022). Data augmentation and transfer learning for brain tumor detection in magnetic resonance imaging. *IEEE access*, *10*, 23217–23233. DOI: 10.1109/ACCESS.2022.3154061

[41] Bacanin, N., Bezdan, T., Venkatachalam, K., & Al-Turjman, F. (2021). Optimized convolutional neural network by firefly algorithm for magnetic resonance image classification of glioma brain tumor grade. *Journal of real-time image processing*, *18*(4), 1085–1098. DOI: 10.1007/s11554-021-01106-x

[42] Ekong, F., Yu, Y., Patamia, R. A., Feng, X., Tang, Q., Mazumder, P., & Cai, J. (2022). Bayesian depth-wise convolutional neural network design for brain tumor MRI classification. *Diagnostics*, *12*(7), 1657. DOI: 10.3390/diagnostics12071657

[43] Fayaz, M., Torokeldiev, N., Turdumamatov, S., Qureshi, M. S., Qureshi, M. B., & Gwak, J. (2021). An efficient methodology for brain MRI classification based on DWT and convolutional neural network. *Sensors*, *21*(22), 7480. DOI: 10.3390/s21227480

[44] Misra, S., & Wu, Y. (2020). Machine learning assisted segmentation of scanning electron microscopy images of organic-rich shales with feature extraction and feature ranking. In *Machine learning for subsurface characterization* (pp. 289–314). Gulf Professional Publishing. DOI: 10.1016/B978-0-12-817736-5.00010-7

[45] Mane, D., Khode, O., Koli, S., Bhat, K., & Korade, P. (2023). CNN-based medical image restoration using customized adaptive histogram equalization. *International conference on power engineering and intelligent systems (PEIS)*. (pp. 267–285). Springer. DOI: 10.1007/978-981-99-7383-5_21

[46] Ouchicha, C., Ammor, O., & Meknassi, M. (2020). CVDNet: a novel deep learning architecture for detection of coronavirus (Covid-19) from chest x-ray images. *Chaos, solitons & fractals*, *140*, 110245. DOI: 10.1016/j.chaos.2020.110245

[47] Rehman, A., Khan, M. A., Saba, T., Mehmood, Z., Tariq, U., & Ayesha, N. (2021). Microscopic brain tumor detection and classification using 3D CNN and feature selection architecture. *Microscopy research and technique*, *84*(1), 133–149. DOI: 10.1002/jemt.23597

[48] Khan, M. S. I., Rahman, A., Debnath, T., Karim, M. R., Nasir, M. K., Band, S. S., … & Dehzangi, I. (2022). Accurate brain tumor detection using deep convolutional neural network. *Computational and structural biotechnology journal*, *20*, 4733–4745. DOI: 10.1016/j.csbj.2022.08.039

[49] Pandiselvi, T., & Maheswaran, R. (2019). Efficient framework for identifying, locating, detecting and classifying MRI brain tumor in MRI images. *Journal of medical systems*, *43*(7), 189. DOI: 10.1007/s10916-019-1253-1

[50] Shanjida, S., Islam, M. S., & Mohiuddin, M. (2022). MRI-image based brain tumor detection and classification using CNN-KNN. *2022 IEEE IAS global conference on emerging technologies (GLOBCONET)*. (pp. 900–905). IEEE. DOI: 10.1109/GlobConET53749.2022.9872168

[51] Hamada, A. (2020). *Br35h: Brain tumor detection*. https://www.kaggle.com/datasets/ahmedhamada0/brain-tumor-detection